InterPack2021-72682

Proceedings of the ASME 2021 International Technical Conference and Exhibition on Packaging and Integration of Electronic and Photonic Microsystems
InterPACK2021
October 26-28, 2021, Virtual, Online

IPACK2021-72682

A NOVEL CONCEPT FOR AIR REMOVAL IN TWO-PHASE IMMERSION COOLING SYSTEMS

Eric Peterson[1], Seth Morris[2], Husam Alissa[1], Nicholas Keehn[1], Bharath Ramakrishnan[1], Vaidehi Oruganti[1], Ioannis Manousakis[1], Noah Mckay[2]

[1]Microsoft Corporation, Redmond, WA, USA
[2]D2H Advanced Technologies, Winston-Salem, NC, USA

ABSTRACT

A 10 kW scale model of a decoupled immersion cooling rig is constructed in order to serve as a testbed for immersion cooling, using 3M FC3284 dielectric cooling fluid. A species separator is constructed and demonstrates an ability to remove air from the flowfield before the condensable gases enter the condenser vessel, verified with Schlieren photography. The condenser underperformed significantly compared to initial sizing calculations using the NTU method, and film thickness of FC3284 liquid on the surface of the condenser was determined to be the cause due to low thermal conductivity of the liquid. The average film thickness on the surface of the condenser is calculated. In addition to the performance detriment of the film, air is also shown to reduce the condenser's performance. The height of a transient stratification line is measured and compared against condenser power. Condenser efficacy losses are large and variable based on the concentration of air in the condenser vessel. A low vs high-mounted boiler is investigated. The mounting of the boiler has an effect on how much vapor is lost during a maintenance event. Finally, a comparison of the test rig's overall cooling efficiency is made with various air-cooled datacenters by tracking energy consumption to cool a given IT load. This also translates to a reduction in carbon emissions.

Keywords: Two-phase, immersion cooling, air removal, species separator, noncondensibles, stratification layer, segregated two-phase immersion cooling,

NOMENCLATURE

P	pressure
ρ	density
R	gas constant
T	Temperature
HV	Specific heat of vaporization
$\dot{Q}$	Rate of heat transfer
$\dot{m}$	Mass flow rate
c_p	Specific heat
C	Capacity, equal to $\dot{m}c_p$
ε	Heat exchanger effectiveness
U	Average flow velocity through a cross section
L	Length of pipe
f	Friction factor
D	Hydraulic diameter
Nu	Nusselt number
PW	Pumping power
q	Volume flow rate

1. INTRODUCTION

A segregated two-phase immersion cooling system separates the boiler, where the IT load is introduced to the cooling fluid, and the condenser. The different parts of the system are connected via ductwork. Figure 1 shows a drawing.

The species separator was conceived to mitigate air's performance-hindering effects on the condenser. Air may enter the system during a maintenance procedure. In this event, the lid of the boiler is removed, perhaps to replace a board, but the IT load is not shut down. In this case, vapor may be displaced by air by a number of mechanisms:

- Buoyancy effects, depending on system layout
- Local air currents
- Currents from physically interacting with the local flowfield.

Once air has entered the system, if it is not removed, then it may flow to the condenser, where it reduces the condenser's performance. The reduction in condenser performance is quantified later in this publication.

The species separator is designed to remove the air from the flowfield before it enters the condenser vessel. It was developed using ANSYS Fluent.

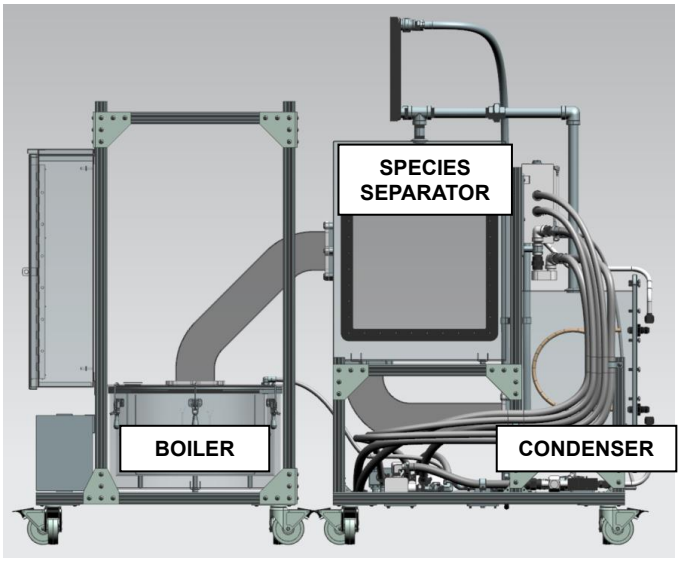

FIGURE 1: LAYOUT OF SEGREGATED TWO-PHASE IMMERSION COOLING SYSTEM

The 10kW scale model of the segregated two-phase immersion cooling system was constructed to provide a scale model testbed for various concepts. Two of these concepts covered in this document are a reduction in cooling fluid loss during a maintenance event, and handling of air during a maintenance event. The scale model further is used to test the efficacy of a species separator. The method of verification of the species separator's operation is qualitative using Schlieren photography to visually correlate the CFD results.

The effect of air on condenser performance is quantified by tracking the stratification layer's height as it passes across the condenser during system purge (purging of air), while simultaneously measuring condenser heat transfer rate. The stratification layer is a visible layer above which is presumed to be mostly air, and below which is presumed to be mostly condensable vapor, though the exact mass fractions of the mixtures above and below are not known. Mass fraction is defined as the mass of the air divided by the mass of the vapor for a given sampled volume. This quantity is locally measured, and not as meaningful over the volume of the entire system.

2. MATERIALS AND METHODS

There are 6 subsections: the mechanical design of the test rig, the condenser sizing, design of the species separator, commissioning, the CFD model, and the Schlieren photography setup.

The test rig and CFD model use 3M™ Fluorinert™ Electronic Liquid FC-3284. Material properties are covered in more detail in the SDS sheet [1]. Basic material properties are as follows:

- Heat of vaporization 105 kJ/kg
- Saturation temperature @ P_{atm} 50C
- Liquid density @ 50C 1710 kg/m^3
- Liquid thermal conductivity @ 50C 0.062 $W/m-K$

2.1 Mechanical Design of the Test Rig

This section covers some of the details of the mechanical design of the test rig. In this section, the overall design is presented (Figure 2 below), a water-side hydraulic circuit diagram for condenser flow and temperature control, and cover some of the details about fabrication of the unit.

Cooling fluid is loaded into the boiler, which simulates the IT load using heating sticks. These sticks are controlled with a PWM signal to the desired rate of heat transfer, using combinations of sticks as heating increases, to all the sticks at 10kW. System input heat can be requested at any value between 0-10kW. Vapor then travels up the inlet duct into the species separator, where any air that may have been introduced in the boiler is allowed to separate out. It then travels through the outlet duct into the condenser vessel. Liquid coolant then drips to the bottom of the vessel and is collected by an in-line gear pump, which pumps the fluid back to the boiler.

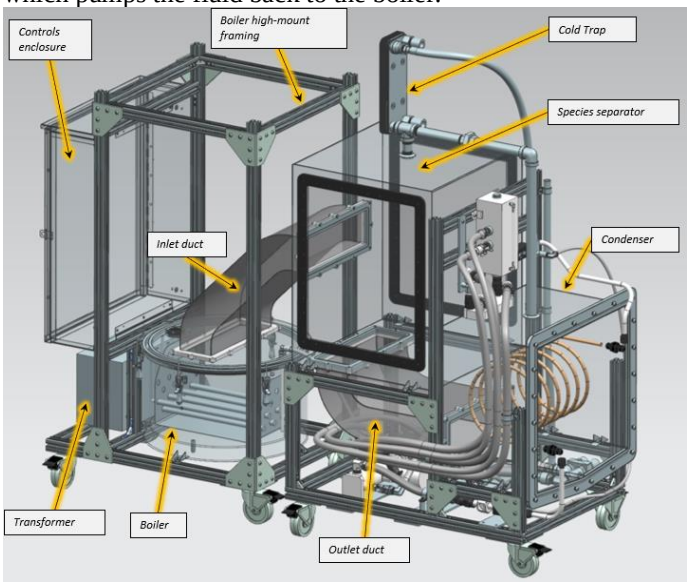

Figure 2: CAD MODEL OF THE TEST RIG WITH COMPONENT CALLOUTS

In both the species separator and the condenser, there are vent pipes that run to a cold trap. The vent pipes serve to equalize pressure to the ambient, and allow an outflow while purging the system of air on startup. The cold trap's purpose is to condense any remaining vapor in the air when it is being purged.

The unit's condenser circuit utilizes a water-to-water heat exchanger, complete with a pump and heater on the condenser side so that inlet water temperature can be controlled. Winston-Salem city water is in the 25-30°C range, but 40°C is not unusual for a water system using a water tower to cool in a hot environment.

The water side sensors are covered in the following list:

- Pressure differential across the coil
- Condenser water inlet temperature

- Condenser water outlet temperature
- Water volume flow rate, using a turbine in-line flow meter.

The water-side hydraulic circuit diagram and sensory for the control system are laid out in Figure 3 below.

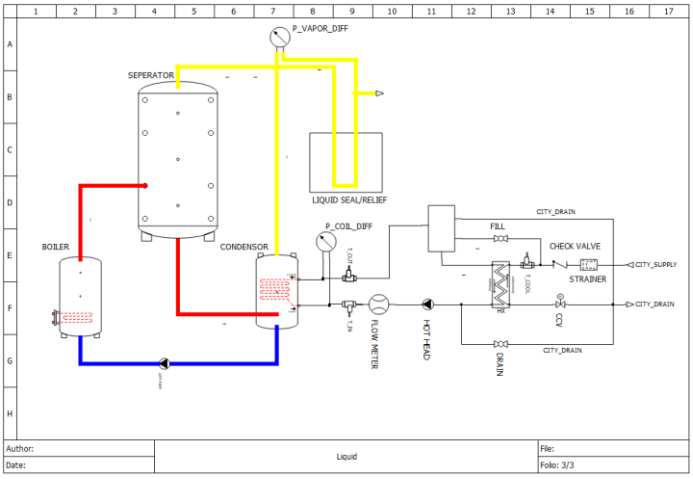

Figure 3: WATER-SIDE HYDRAULIC CIRCUIT DIAGRAM AND SENSORY FOR CONTROL SYSTEM

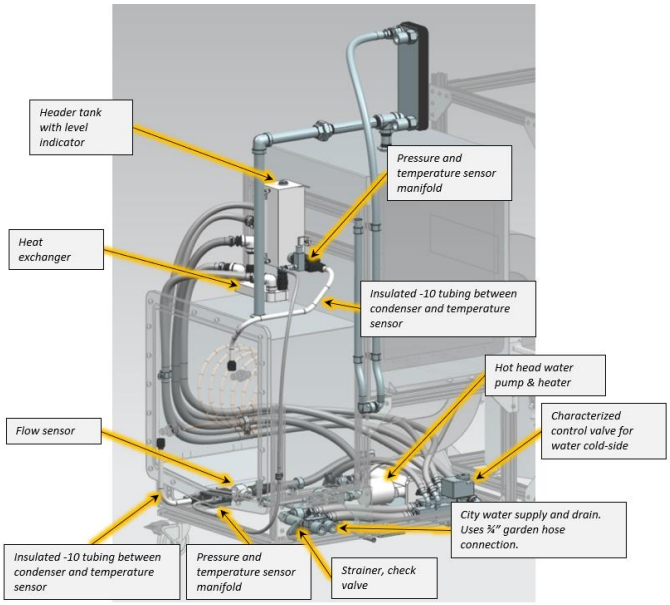

Figure 4: PART CALLOUTS FOR WATER CONTROL SYSTEM

With these sensors, the power requirements, PW to drive flow across the heat exchanger, may be calculated, as well as the rate of heat transfer $\dot{Q}$ using the following equations.

$$\dot{Q} = \dot{m}Cp\Delta T \qquad (1)$$

The pumping power requirements are:

$$PW = q\Delta P \qquad (2)$$

The pressure sensor is differential-type, manufactured by Measurement Specialties, Inc., part number D5154-00005-005PD. It has an accuracy of +-0.25% of span @ 5psi [2].

The temperature sensors are a class A sensor with a max error of 0.25°C at 50°C.

And the flow sensor is a turbine in-line type flow meter from Universal Flow Monitors. The model number is TM0050-1/2, and it has a +- 1% accuracy over the range with a +-0.1% repeatability over its range [3].

The water control system uses a closed-loop cooling arrangement with a pump and heater on the condenser side of the circuit. This arrangement allows for better condenser inlet temperature control. There is also a header tank which allows for filling of the closed loop side, and allows for system bleeding to eliminate air bubbles.

On the city water side of the circuit, there is a strainer and check valve, which flows up to the water-to-water heat exchanger. Following that is a characterized control valve which controls the city-water side flow rate.

The boiler, shown in Figure 5, uses a double-wall spun casing with a quick-release lid. Heaters are installed in a basket which sits at the bottom of the tank.

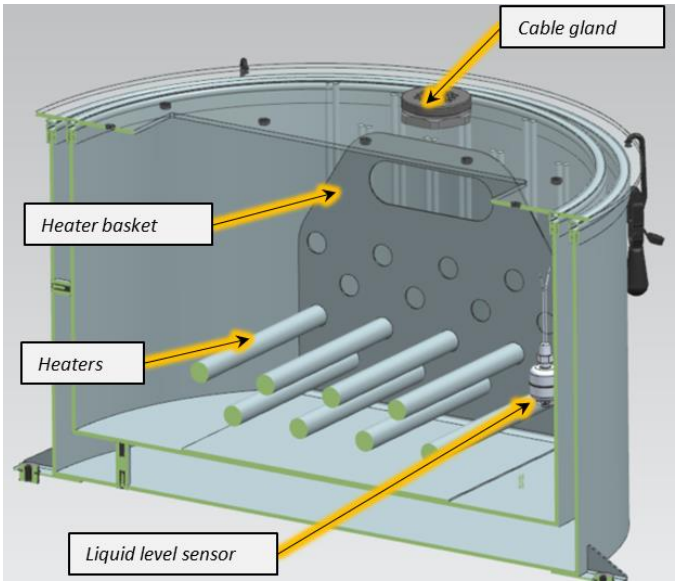

Figure 5: CROSS SECTION OF BOILER VESSEL

The technical operation of the species separator will be covered in Section 2.3 “Design of the Species Separator”. The mechanical design is covered in the following paragraph. Figure 6 shows the mechanical design of the species separator.

The species separator is designed to ingest 5 gallons of air before the condensable vapor is sent to the condenser vessel. The dimensions of the inner walls were determined with a design

study in CFD. The vessel has windows on either side, bonded and riveted to the walls. These windows allow for Schlieren photography to be performed, which is used as a means of correlation to CFD. The flanges are welded from the inside, providing a vapor-tight seal, because vapor will not be allowed up to the bolt holes. Flange bolt holes are blind holes to disallow any leak path that would occur with a through hole. Finally, flanges have o-ring grooves for a tight, serviceable, gasketed connection.

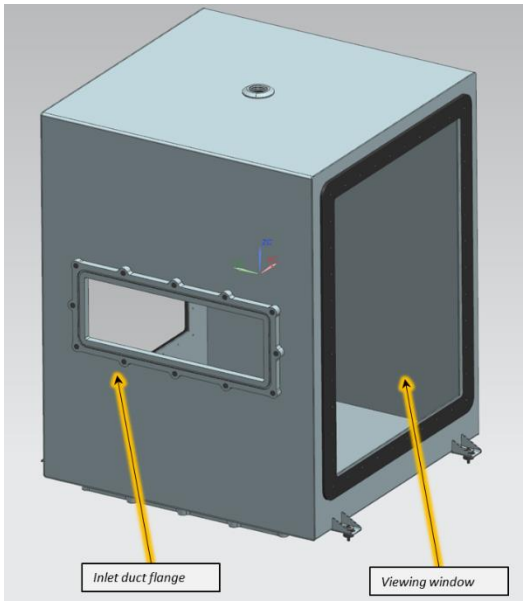

Figure 6: SPECIES SEPARATOR

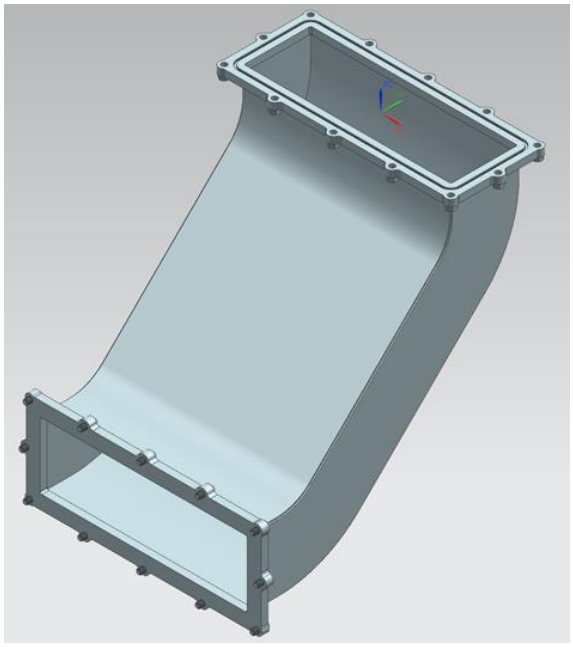

Figure 7: OUTLET DUCT

Ductwork geometry is determined in CFD and was designed to reduce air/vapor mixing if air is introduced in the boiler due to removal of the lid. This reduction in mixing improves species separator performance. The reduction in mixing is achieved by using a broad radius for the bends, and an incline for the duct to slow any buoyant flow of air. CFD was used for flowfield visualization to check that the bend radii were broad enough for fully attached flow. Flow visualization was also used in choosing the slope of the inclined section of the duct. It was ensured that a "bubble" of air didn't break through the surrounding vapor, and that a sheet of air stayed attached to the upper wall. Work should be done to quantify the effects of the downhill slope that the air would take if it gets ingested in the high-mount boiler configuration.

The material is 5052-H32 welded and formed aluminum walls. 5052-H32 has a high degree of formability but has a higher yield strength than either 3003-O or 6061-O. The –O heat treatment reduces the yield strength of those respective alloys by a factor of 2-5 over a –T6 heat treatment. Flanges are 6061-T6 for good machinability. They are 0.500" thick to mitigate warpage during welding.

The operating pressure is kept inside a +-1kPa band due to the low yield strength of the aluminum and the square shape of the components.

2.2 Condenser Sizing

The condenser was sized using a D2H-written Octave code, using the NTU method. Given the fluid material properties, water inlet temperature, and hot side vapor temperature, and assuming a smooth tube bore, as well as assuming an infinitely large capacity *C*, this code will calculate the following:

- Friction factor
- Water side pumping power, using the Darcy-Weisbach equation for pressure drop
- Water side outlet temperature
- Hot side "outlet" temperature. For a condenser, this will be the saturation temperature since phase change is an isothermal process
- Heat exchanger effectiveness
- Actual rate of heat transfer $\dot{Q}$

The Darcy-Weisbach equation [4] is used to calculate the pressure drop in a straight, level, uniform pipe:

$$\Delta P = \frac{\rho U^2 f L}{2D} \tag{3}$$

In the design of the condenser, a single-cooling circuit arranged in a coil was selected. The coil has a large helix diameter compared to the hydraulic diameter, and the Darcy-Weisbach equation was assumed to be applicable. Additionally, the inlets and outlets are in the same plane.

Note that the thermal conductivity of the copper condenser tube is not accounted for in the heat exchanger model. Since the copper is thin and highly conductive, it is assumed that its resistance to be negligible.

Once the actual rate of heat transfer $\dot{Q}$ is determined, then the geometry of the condenser tube may be optimized for

pumping power. There are a number of variations in diameter, flow rate, and pipe length that will satisfy the heat transfer requirements. The in-house developed flow optimizer loops over diameter as well as length, solving for the flow rate required to satisfy the desired rate of heat transfer; in this case, 10kW.

The output of this code gives generate 2 plots of interest. The first compares pumping power vs coil length for a given tube diameter.

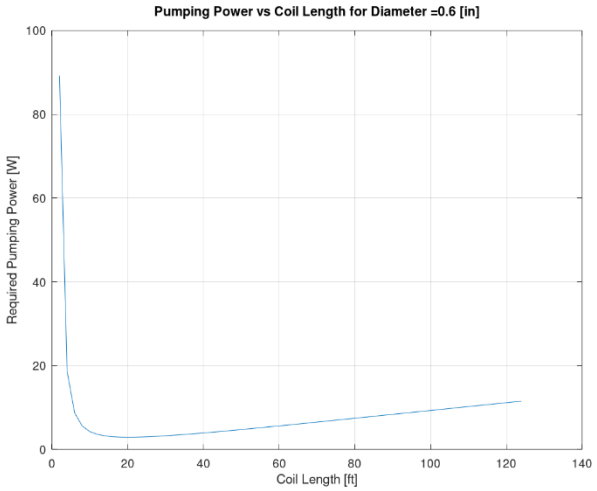

Figure 8: PUMPING POWER VS COIL LENGTH FOR DIAMETER 0.6"

Note that in Figure 8 above, there exists a minimum. To the left of this minimum (decreasing tube length), pumping power increases at a substantial rate. Since the tube is so short, the flow rate requirements are enormous, requiring substantial pumping power to achieve the required rate of heat transfer. To the right of the local minimum (increasing tube length), the flow rate continues to decrease, but the viscous losses in the water have started to dominate.

For each of these plots, there exists a local minimums that may be plotted, to investigate the sensitivity to diameter:

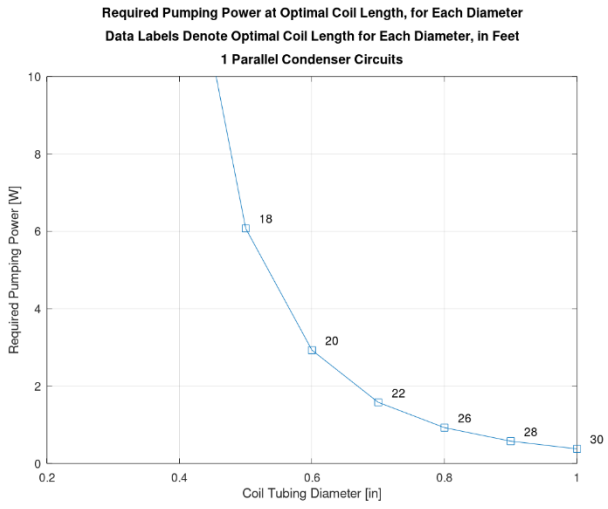

FIGURE 9: REQUIRED PUMPING POWER VS COIL TUBING DIAMETER, OPTIMAL LENGTH FOR EACH DIAMETER

Note that the larger the diameter, the longer the length required. This phenomenon is due to the velocity of the flow inside the tube reducing as diameter increases, which requires a slightly longer length to achieve the same heat transfer. Nevertheless, the least pumping power is achieved by the largest tube diameter because the viscous losses are much lower for the lower water-side velocity. For this case, 5/8" tubing at 20' long is selected.

2.3 Design of the Species Separator

A diagram of the species separator is detailed in Figure 10 below.

The species separator takes advantage of the large difference in density between air and FC-3284 vapor. Note that other two-phase immersion cooling fluids have similar vapor densities to FC-3284. As FC-3284 is considered an ideal gas near atmospheric pressure, and solving for density at the saturation temperature,

$$\rho = \frac{P}{\frac{R}{M}T} \qquad (1)$$

Where $P = 101{,}325\,Pa$, $R = 8.314\,J/K\,mol$, $M = 0.299\,kg/mol$, and $T = 323.15\,K$. The density is $\rho_{FC3284} = 11.28\,kg/m^3$

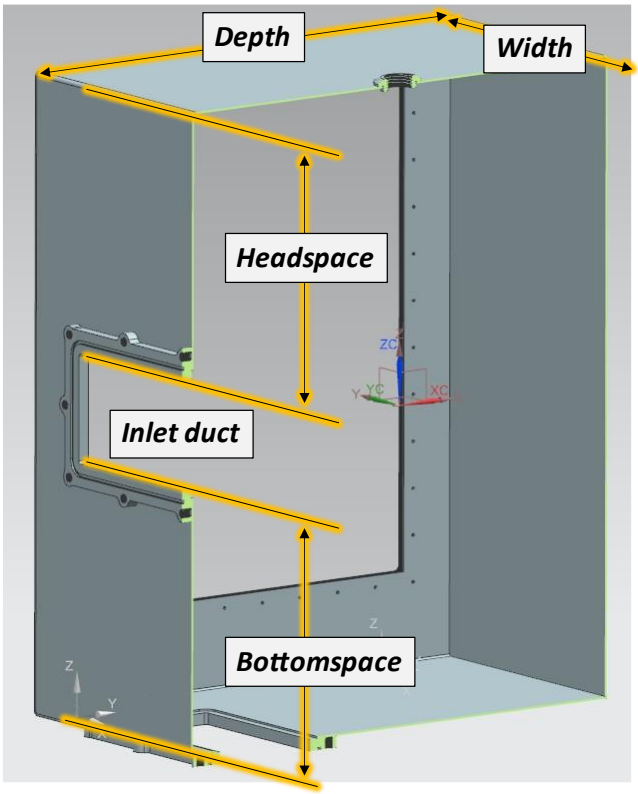

FIGURE 10: DIAGRAM OF SPECIES SEPARATOR DETAILING ITS COMPONENTS

For air, $R/M = 287.06 J/kg\,K$. The density is $\rho_{air} = 1.09\,kg/m^3$. In the case of FC-3284 at saturation temperature, the density ratio is 10.3.

With this large of a density ratio, it was hypothesized that air may be allowed to separate from the flowfield before it enters the condenser vessel by allowing the buoyant forces to dominate. This theory is accomplished by:

- Sizing the cross sectional area of the ductwork from the boiler to the species separator such that the duct flow is <=0.25 m/s.
- Allowing sufficient headspace above the inlet duct for the air to collect. The volume of the headspace as a ratio of the maximum volume flow rate is 10.73 [1/s].
- Allowing sufficient volume in the separator for the flow to diffuse to near-stagnation. The volume of the species separator as a ratio of the volume flow rate is 25.54 [1/s].
- Orienting the exit ductwork such that the flowpath from the inlet must make a 90° turn downwards, giving ample time for the air to separate out. The outlet to the species separator must be near the wall of the inlet duct to force the flow to take a 90° turn as opposed to a lesser angle when the flow forms a straight-line, free-stream jet between the ducts.

The above list was generated using an iterative design approach and ANSYS Fluent as the solver.

The vapor flow rate can be found by using the specific heat of vaporization and the applied IT load. In this case, $HV = 105{,}000 J/kg$ and $\dot{Q} = 10{,}000 J/s$. Thus, $\dot{m} = 0.095\,kg/s$. For a nominal velocity of 0.25 m/s, the cross-sectional area must then be $0.034\,m^3$.

The inlet ductwork must be smooth and avoid abrupt changes in area which would cause severe adverse pressure gradients giving rise to flow separation. A fully attached flow will reduce mixing of the air and condensable vapor.

2.4 Commissioning

Error and repeatability are calculated for each of the following subsystems: boiler power, condenser power, condenser pumping power.

Error was established using the error propagation theory via the uncertainties Python package [5]. The repeatability is also established using the same package. The published sensor accuracies seed the uncertainty calculations.

The largest contribution to error in the boiler power is the current measurement. The largest contribution to error in the condenser power is the temperature measurement. This creates an error floor at a small ΔT. It would be possible to use a bridge measurement technique to directly measure ΔT instead of measuring two individual temperatures. The flow meter contributes very little error to the condenser power measurement. The largest contribution to error in the condenser pumping power is the flow rate measurement.

Figure 11 plots the boiler power error, condenser power error, and condenser pumping power error. Figure 12 plots the repeatability for the boiler power, condenser power, and condenser pumping power.

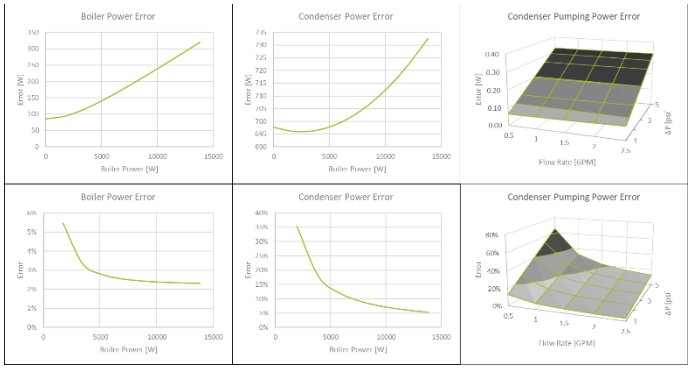

Figure 11: ERROR PLOTS FOR BOILER POWER, CONDENSER POWER, AND CONDENSER PUMPING POWER

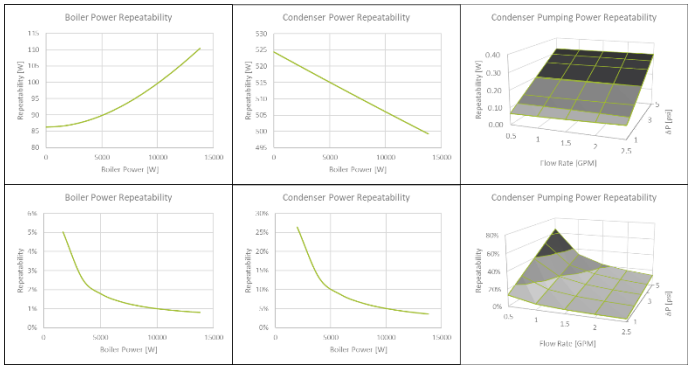

Figure 12: REPEATABILITY PLOTS FOR BOILER POWER, CONDENSER POWER, AND CONDENSER PUMPING POWER

To keep boiler power error below 5%, one must run above 2kW boiler power. At 4kW boiler power, which is the steady state maximum power operation (hindered by condenser performance, discussed later), boiler power error is about 3%. Condenser power is much larger than boiler power, and at 3kW condenser power there is approximately 22% error. More precise, expensive temperature sensors will improve this error. Pumping power error is 7% at a flow rate of 3 GPM and a pressure drop of 3psi, which corresponds to 3kW condenser power. Largest pumping power error occurs at large pressure differentials and low flow rates.

Boiler power repeatability is 2.2% at 4kW boiler power. Condenser power repeatability is 16% at 3kW condenser power. Better temperature sensors will improve repeatability. At 3GPM and 3psi pressure drop, the repeatability of condenser pumping power is 7%.

2.5 The CFD Model

The CFD model was used to design the species separator, and as such, there was no boiling or condensation model. A velocity boundary condition is set at the inlet duct, with a pressure-outlet on the outlet duct to set base pressure of the system. The solution uses a species transport model and a

mixture template available in ANSYS Fluent to model the interaction of the individual species.

The species separator is designed to ingest 5 gallons of air while minimizing the mass fraction of air flowing out of the outlet. Ideally, no air travels out of the outlet as that ends up at the condenser.

The mass flow rate is set by the latent heat of vaporization and the desired boiler power. For this case, 10kW boiler power is selected. FC3284 has a latent heat of vaporization of $105\,kJ/kg$, which equates to $0.095\,kg/s$. The density is $11.28\,kg/m^3$, so the volume flow rate is $8.422E-03\,m^3/s$. At $0.046\,m^2$ of cross sectional area, the velocity is $0.183\,m/s$.

The inlet velocity is 0.25 m/s so the flowfield is modeled as laminar, and with a transient formulation.

The solution was initialized using hybrid initialization for a reasonable guess at the flowfield before the Navier-Stokes equations are solved.

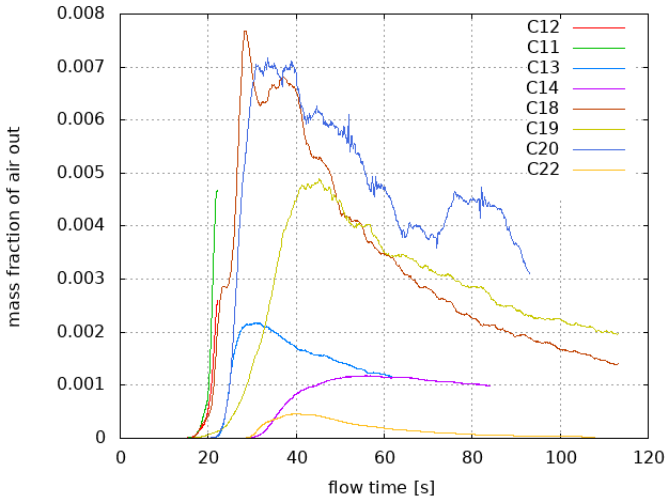

Figure 13: MASS FRACTION OF AIR OUT VS FLOW TIME FOR VARIOUS ITERATIONS OF SPECIES SEPARATOR GEOMETRY

The solution is run until steady state conditions are reached before injecting air. A slug of air is then injected at the same velocity, at 100% mass fraction, until 5 gallons ($0.0189\,m^3$) is reached. At $8.422E-03\,m^3/s$ volume flow rate, the solution must run for 2.24 sec of physical time until the switch back to 100% vapor occurs.

Several design iterations were performed (Cases C11-22), which are plotted in Figure 13 above. These design iterations consisted of changes in headspace volume, width, height, depth, and bottom space volume. In this figure, mass fraction of air out is plotted vs physical time. Note that as the geometry of the species separator is optimized, the mass fraction of air out is reduced significantly. For the best case, there was a 0.00045 mass fraction of air out at peak, occurring 25s after initial injection of air.

A snapshot of the air filtering to the headspace of the species separator is available in Figure 14 below. The air collecting in the headspace of the vessel is observed, along with tumbling and mixing. The mixing causes some dilution of the air with condensable vapor.

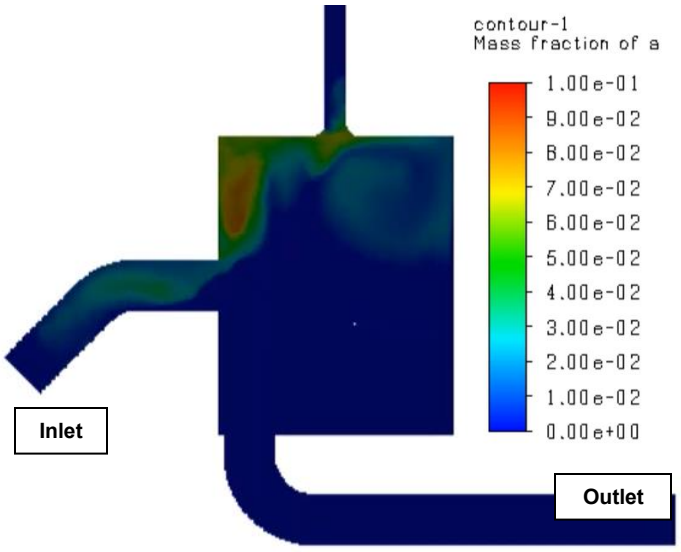

Figure 14: SNAPSHOT OF SPECIES SEPARATOR IN OPERATION (Case C22)

2.6 Schlieren Photography Setup

Schlieren photography was used to visualize the air separate from the FC3284 inside the species separator. It was used to verify the operation of the species separator.

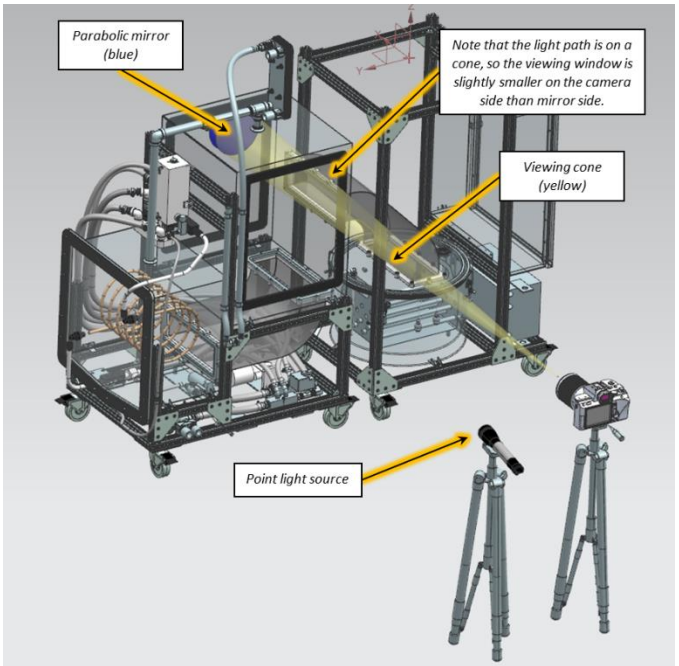

Figure 15: SCHLIEREN PHOTOGRAPHY SETUP

A single-mirror black and white Schlieren photography setup was chosen as the method of flow visualization to verify the operation of the species separator as well as correlation of the

CFD model. Schlieren photography is well understood [6], and this publication only aims to discuss the specific challenges of using Schlieren photography on a pressurized vessel with a condensable vapor inside. Schlieren operates on variations of density along a light ray, where varying densities will refract the light differently. Schlieren is a qualitative verification of the species separator's operation.

The setup is shown in Figure 15 above. In order to see inside the species separator, viewing windows were added to the sides of the vessel. The 8" parabolic mirror is mounted to the chassis of the system, just on the other side of the 2nd viewing window. The camera, point-light source, and razor blade are at the bottom of the figure.

The specific challenges are listed below:

- The viewing cone does not produce data exactly normal to the surface of the viewing windows, and thus, the further away from the camera, the larger the area of data that is captured along the light rays. A dual mirror setup could rectify this problem, but would be more difficult to set up around this specific geometry. In this geometry, it is expected that the flow be 2D-dominant, but with the single mirror setup, it must be noted that data is along a light ray, which is not normal to the surface (except the ray at the center of the mirror).
- Condensation on the viewing windows made the Schlieren photography impossible. The windows were brought to above saturation temperature with heated blankets for approximately 2 minutes prior to photography, with the system running at steady state. The available photography time before condensation reappeared was less than 60 seconds.
- Pressure inside the vessel must be carefully set. Even a 100 Pa deviation from ambient pressure causes the viewing windows to bow enough to divert the light rays such that the Schlieren photography becomes unattainable. The operating pressure was set to 10Pa above ambient to ensure no leakage of outside air into the system. Pressure is set by the balance of boiler power to condenser power.
- Note that under normal operation, operating pressure is limited to a +-1kPa gauge band. These small changes in pressure do not have a measurable effect on the saturation temperature of the vapor nor do they have substantial effect on the density changes due to the ideal gas law. It is then concluded that the photography is being performed during well-represented system conditions.

Video was taken of air being injected into the inlet duct and watching it rise upwards in the species separator. The results of this test are discussed in Section 3.2.

The mirror is set to the upper right corner of the viewing window so that the air flowing upwards into the headspace of the species separator may be observed.

3. RESULTS AND DISCUSSION

The results and discussion section covers 5 subsections: Condenser Performance Reduction Due to Film Thickness, Schlieren Results, Effect of Air on Condenser Performance, and High vs Low Mount Boiler.

3.1 Condenser Performance Reduction Due to Film Thickness

The condenser coil underperformed by about 1/3 of the intended value. It was designed for 10kW of heat rejection, but in fact can only achieve about 3500W of heat rejection. The overlying cause of the severe underperformance is the liquid FC3284 film, which has a low thermal conductivity. This film thickness was not accounted for in the condenser sizing code. It can now be added, as from this experiment, the average film thickness for this geometry has been modeled. However, this average film thickness will be a function of the condenser geometry as the way the film flows along the surface is geometry and surface treatment dependent.

It was determined that the film was the cause of the underperformance via the following analysis. First, the condenser-side temperature of the film is calculated based on an average film thickness of 0.005" (0.127mm) and assuming the vapor-side film temperature is at saturation (50C). This calculation was performed to check the sensitivity of the inner temperature to film thickness. This calculation shows that the inner temperature is significantly reduced with a small 0.005" film thickness and a thermal conductivity of 0.06 $\frac{W}{mK}$. Then, the Log-Mean Temperature Differential (LMTD) is used to calculate the average condenser-side film temperature, and then use this result to calculate an average film thickness.

Consider the conduction equation:

$$\dot{Q} = \frac{kA\Delta T}{t} \qquad (2)$$

Where $\dot{Q}$ is the rate of heat transfer, k is the thermal conductivity of the film, A is the surface area of the condenser, ΔT is the temperature delta between the inner and outer surfaces (vapor side and water side), and t is the thickness of the film. If $\Delta T = (T_o - T_i)$, then one may rearrange Equation 2 to solve for the inner temperature (condenser-side) T_i.

$$T_i = T_o - \frac{\dot{Q}t}{kA} \qquad (3)$$

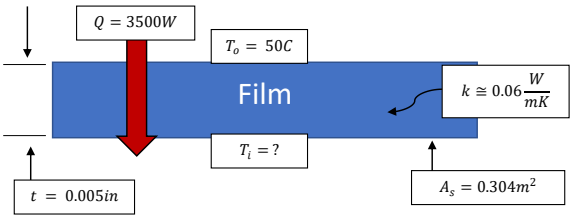

Figure 16: DIAGRAM OF FILM THICKNESS HEAT TRANSFER ANALYSIS WITH A KNOWN FILM THICKNESS

Below are the following assumptions and inputs:

- Outer film temperature is at saturation temperature, or 50C
- Film thickness set to 0.127mm for a sensitivity check, before proceeding to LMTD method.
- Thermal conductivity of the film is set to $0.06\frac{W}{mK}$
- Surface area is calculated to be $0.304m^2$ for the condenser.
- Using a rate of heat transfer of 3500W.
- Only considering the film to conduct and ignoring any convection heat transfer. Since the film is thin, the viscous forces are high, and this assumption is thought to be reasonable.

With the above assumptions and inputs, the inner film temperature is 25.6C. During testing, the water inlet temperature to the condenser was about 35C. Since condensation is being achieved, it is known that the average film thickness must be even thinner than 0.005" so that the inner film temperature must be higher than 35C.

The average film thickness can be calculated, but an average inner film temperature must be known. This value can be estimated using the LMTD formulation to find an average wall temperature based on water inlet and outlet temperatures.

For this calculation, data was gathered at a specific set point, measuring condenser power as well as water inlet and outlet temperatures. This is enough data to calculate an average condenser surface temperature using LMTD of the water inlet and outlet temperatures and assuming the copper is the same temperature as the water. Since the wall is thin, and the thermal conductivity of copper is about 4 orders of magnitude higher than FC32847, it is felt that this to be a valid assumption. An average thermal conductivity of the FC3284 liquid between 35-50C is used.

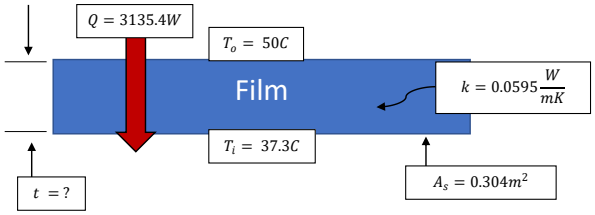

Figure 17: DIAGRAM OF FILM THICKNESS HEAT TRANSFER ANALYSIS USING LMTD FOR INNER FILM TEMPERATURE, SOLVING FOR FILM THICKNESS

The LMTD equation is as follows:

$$LMTD = \frac{\Delta T_A - \Delta T_B}{ln\left(\frac{\Delta T_A}{\Delta T_B}\right)} \quad (4)$$

And the equation corresponds to Figure 18 below. In this figure, the red line is the saturation temperature of 50C, and the blue line is the water temperature at inlet and outlet.

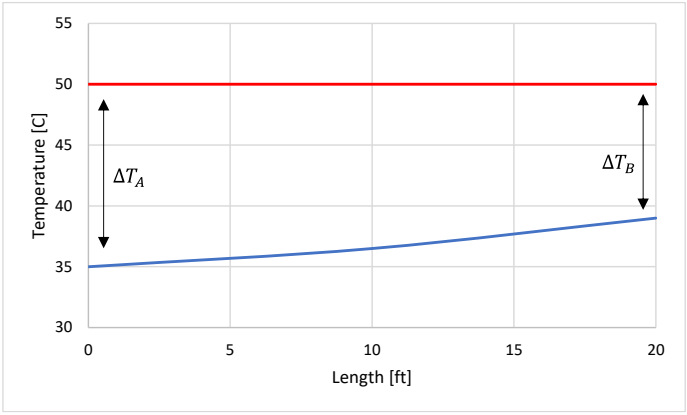

Figure 18: DIAGRAM SHOWING TEMPERATURE DIFFERENTIALS FOR LMTD EQUATION

The values of condenser power, water inlet and outlet temperatures, saturation temperature, average thermal conductivity of FC3284, and coil surface area are summarized in Table 1. These values are used to solve for the average film thickness. The average film thickness is solved to 0.002" based on an average condenser surface temperature of 37.3C. Note that there is a 12.7C loss in temperature delta with which to transfer heat because of the presence of the poor conducting film.

Table 1: INPUTS FOR FILM THICKNESS ANALYSIS USING LMTD TO ESTIMATE INNER FILM TEMPERATURE. THESE ARE MEASURED VALUES FROM A STEADY STATE TEST.

Variable	Value	Units
Boiler Power	4529.6	[W]
Condenser Power	3135.4	[W]
Water Inlet Temp	35.29	[C]
Water Outlet Temp	39.12	[C]
Water Mass Flow Rate	0.1954	[kg/m^3]
Saturation Temp	50	[C]
LMTD	12.70	[C]
Average condenser surface temp	37.30	[C]
Average thermal conductivity from 35-50C	0.0595	[W/m-K]
Coil diameter	0.625	[in]
Coil length	20	[ft]
Coil surface area	0.304	[m^2]
Coil wall thickness	0.0625	[in]
Average film thickness	**0.002**	**[in]**

In Table 1, the difference between boiler power and condenser power is due to heat flux through the walls of the unit.

It is important to note that though there may be convective heat transfer in the film, the presence of the film is the major

finding in this work. When not accounted for, the NTU code undersizes the condenser to 1/3 the intended value. Future work should include the heat transfer through the film when sizing the condenser, with either CFD or an addition to the code.

It is not currently known if Schlieren photography can be used to measure the film thickness, nor has it been investigated. CFD is being employed to better quantify the film thickness.

3.2 Schlieren Results

The Schlieren results qualitatively verified species separator operation. The incoming airflow was observed to be flowing towards the top of the species separator, and after some tumbling time, it settled out. Figure 19 and Figure 20 show two snapshots of the Schlieren imaging, one just after the air is injected, and one as the mixture has settled.

With this result, CFD was regarded as a useful development tool in the refinement of the species separator design.

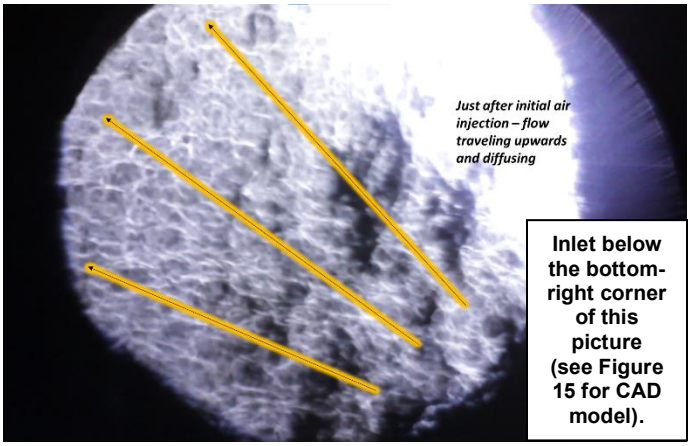

Figure 19: JUST AFTER INJECTION OF AIR, FLOW IS TRAVELING VERTICALLY AND DIFFUSING

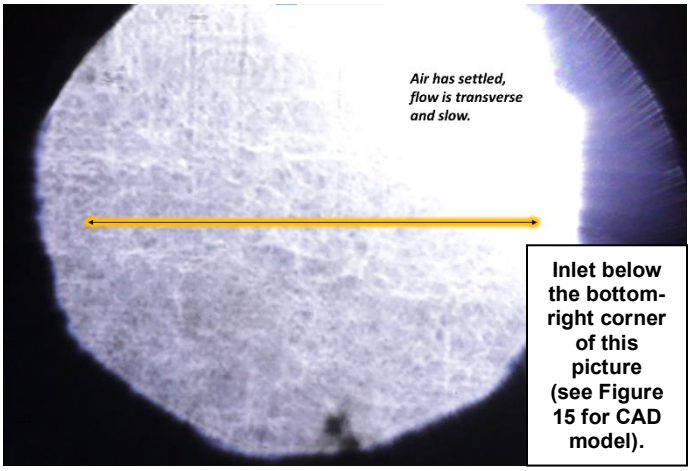

Figure 20: AIR HAS SETTLED AT THE TOP OF THE SPECIES SEPARATOR, THE FLOW IN THE VIEWING WINDOW IS SLOW AND TRANSVERSE

3.3 Effect of Air on Condenser Performance

Air has a considerable effect on performance of the condenser. A transient test was run, tracking the stratification layer height along with condenser rate of heat transfer.

The stratification layer is a visible layer above which is presumed to be mostly air, and below which is presumed to be mostly vapor. The actual mass fractions of the mixtures are not known. Wall temperature of the aluminum condenser vessel shows a couple degrees above ambient above the stratification layer, and a couple degrees below saturation below the stratification layer using a laser thermometer.

To test the air's impact on condenser performance, heat transfer across the condenser was measured while measuring the height of the stratification layer during a system purge. A system purge is when the system is starting fresh, when the system is full of air and the air needs purged out to fill the volume with vapor. The results of this test are presented in Figure 22 below.

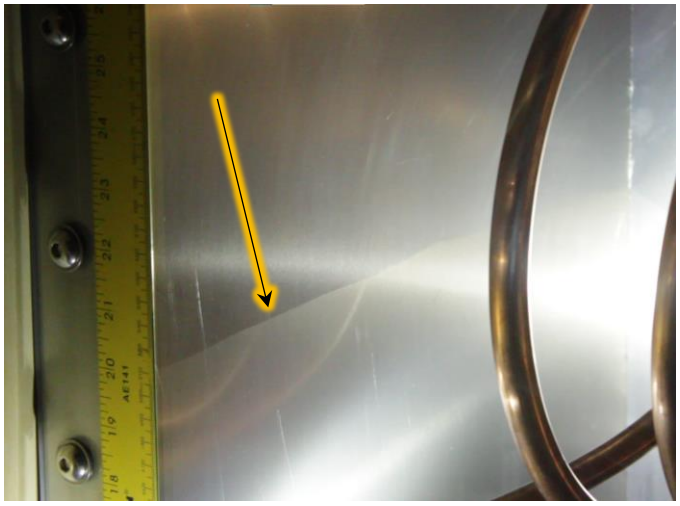

Figure 21: PICTURE OF THE STRATIFICATION LAYER DURING SYSTEM PURGE

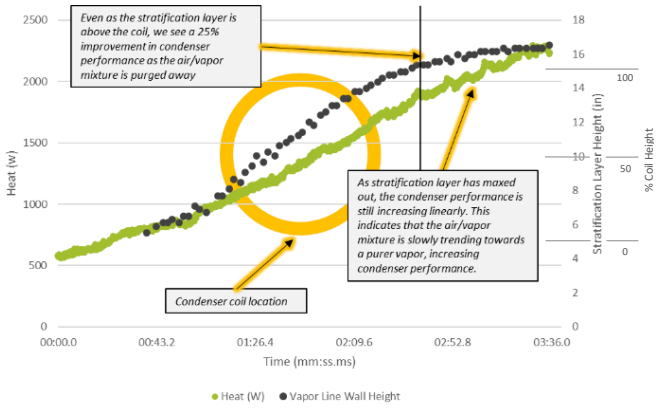

Figure 22: STRATIFICATION LAYER HEIGHT AND CONDENSER POWER DURING A SYSTEM PURGE

The effect of air on condenser performance is evident in Figure 22. Interestingly, when the stratification layer is above the coil and at maximum height, the condenser still is seeing an increase in performance. This indicates that there is likely an air/vapor mixture below the stratification layer, and further purging is required to ensure near-100% vapor around the condenser.

The test did not run until steady state on the condenser. Maximum condenser power is 2300W for this test, but the condenser is capable of 3150W when fully purged. An important observation from this test is that air is capable of reducing condenser performance significantly. Though the exact mass fraction of air across the stratification layer is not known, when the stratification layer is below the coil, the coil can generate about 700W of heat transfer, but at maximum performance, fully purged of air, it is about 3200W. It is plausible that there is at least some vapor above the stratification layer and that some phase change may be occurring. Condenser performance is therefore highly linked to air concentration, and further work should be carried out to understand the exact mass fractions of air and the corresponding condenser performance. Furthermore, because of buoyancy effects, air can be trapped, depending on geometry. Thus, geometry will have an effect on the way air reduces condenser performance. This phenomenon highlights the need to separate the air out before it enters the condenser vessel, but also to create a system that has the ability to purge entirely, and not trap air that will linger during normal operation.

3.4 High vs Low Mount Boiler

The high vs low mount boiler test was performed in order to investigate gravity's effect on fluid loss during a maintenance event. In a maintenance event, the boiler's lid is removed and thus the internal flowfield is exposed to air. Because the density of FC3284 vapor being so much higher than air, with a low mounted boiler, it is hypothesized that gravity would allow the vapor to fall out of the ductwork and system, while air would replace it.

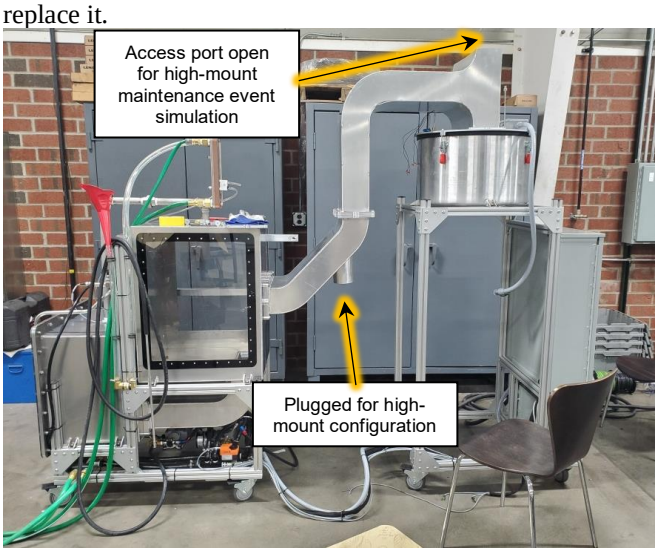

Figure 23: HIGH MOUNT BOILER CONFIGURATION DURING FITMENT MOCKUP

In the simulated maintenance event, the access port was removed on both the low and high mount boiler for 5 minutes, while the boiler stayed in operation. It is important to note that the access ports are different between high and low mount configuration. Figure 23 illustrates the high-mount boiler configuration and shows the rectangular access panel that was removed for this test. For the low-mount configuration, the circular access port in the duct is removed. This configuration is shown in Figure 24.

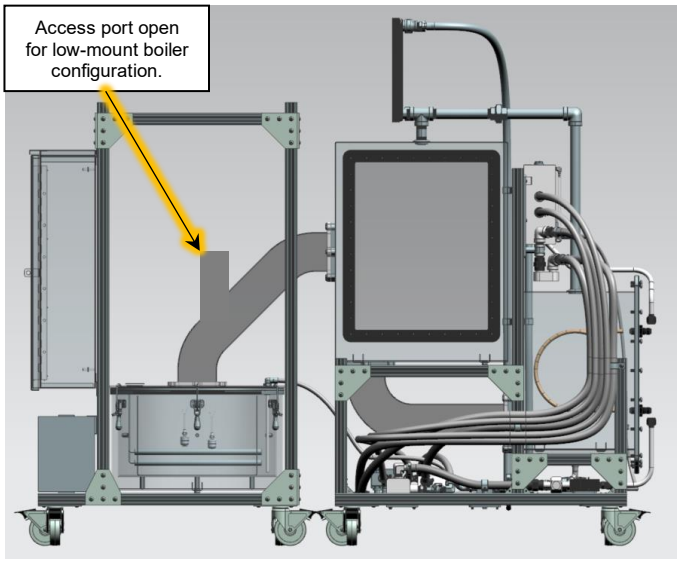

Figure 24: ACCESS PORT FOR LOW-MOUNT BOILER CONFIGURATION DURING THE SIMULATED MAINTENANCE EVENT

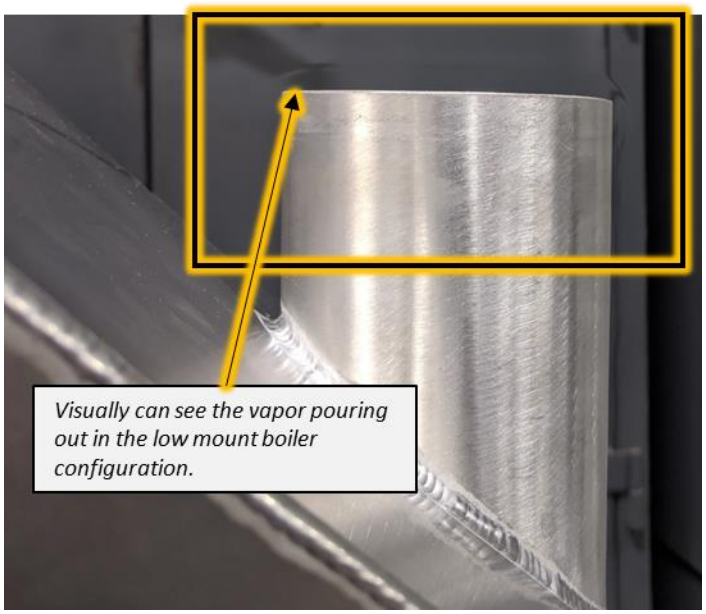

Figure 25: ACCESS PORT OPEN IN THE LOW MOUNT BOILER CONFIGURATION SHOWING VAPOR POURING OUT OF THE ACCESS PORT CAUSED BY BUOYANT FORCES

It was attempted to measure fluid loss during this test, so after the test was complete, the system was shut down, all condensible vapor condensed via the condenser, and all liquid FC3284 was pumped back to the boiler vessel. Then, a dip-stick was used to measure ending fluid volume. This procedure was not repeatable enough to quantitatively determine the amount of fluid loss. The standard deviation in fluid height measurement was larger than the amount of fluid lost. This measurement is complicated by the fact that there is still some residual fluid in the system; though it was attempted to pump all the fluid back, some may remain in the return lines or as droplets on the walls inside the system.

However, it was possible to make a qualitative determination of the better arrangement. When the access cover is open, the vapor flowing out of the open ductwork on the low-mount boiler is very apparent. This vapor was not pouring out of the ductwork on the high mount boiler.

4. CONCLUSION

The species separator was shown to qualitatively operate, and coupled with the observed reduction in condenser performance, it was concluded that air handling before the air meets the condenser is critical. More work needs to be performed in quantifying exactly what local mass fraction of air reduces condenser performance. Air's concentration near the surface of the condenser will be best understood with more complex understanding of the local flowfield and the balance of buoyant vs kinetic forces.

The Schlieren photography, once the technical challenges of operation were overcome, proved meaningful in visualizing the air column as it is injected in the system during a simulated maintenance event. The visualization of the air ensured the species separator was operating as intended (air removal before the condenser). It is important to further note that condenser performance did not drop when the air passed through the system.

Qualitatively, it was concluded that the high-mount boiler configuration is preferred. There was no visible spillage of vapor through the access port in the high mount configuration while there was significant spillage in the low-mount configuration.

The CFD is used for ensuring duct bend radii were adequate and choosing a slope that kept the air from forming a bubble and causing vapor/air mixing. Furthermore, it was a necessary tool in determining the dimensions and duct inlet-outlet layout of the species separator.

It is discovered in this project that liquid film thickness on the surface of the condenser has a massive reduction in performance of the condenser. It is thus necessary to recommend that more advanced modeling of the condenser is necessary early in the design phase. Tools such as CFD with an Eulerian multiphase solution would be more appropriate.

REFERENCES

[1] 3M, Retrieved June 2021, https://multimedia.3m.com/mws/mediawebserver?mwsId=SSSSSuUn_zu8l00xl821P8_SOv70k17zHvu9lxtD7SSSSS--

[2] TE Connectivity, Retrieved April 2021, https://www.te.com/commerce/DocumentDelivery/DDEController?Action=srchrtrv&DocNm=D5100&DocType=DS&DocLang=English

[3] Universal Flow Monitors, Retrieved April 2021, https://www.flowmeters.com/files/Turbine%20Meters/TurbineTM_071018.pdf

[4] Blevins, Robert D. *Applied Fluid Dynamics Handbook*, 2003.

[5] Python, Retrieved June 2020, https://uncertainties-python-package.readthedocs.io/en/latest/

[6] NASA, Retrieved September 2020, https://www.grc.nasa.gov/www/k-12/airplane/tunvschlrn.html